Applied Surface Science 432 (2018) 110–114

Contents lists available at ScienceDirect

Applied Surface Science

journal homepage: www.elsevier.com/locate/apsusc

Full length article

Networks of non-planar molecules with halogen bonds studied using scanning tunneling microscopy on Au (111)

Min Hui Chang[a], Won Jun Jang[a], Min Wook Lee[a], Un Seung Jeon[a], Seungwu Han[b], Se-Jong Kahng[a,*]

[a] Department of Physics, Korea University, 145 Anam-ro, Seongbuk-gu, Seoul 02841, Republic of Korea
[b] Department of Materials Science and Engineering, Seoul National University, 1 Gwanak-ro, Gwanak-gu, Seoul 08826, Republic of Korea

ARTICLE INFO

Article history:
Received 10 October 2016
Received in revised form 24 January 2017
Accepted 25 January 2017
Available online 27 January 2017

Keywords:
Molecular nanostructures
Self-assembly
Scanning tunneling microscopy
Halogen bond
Non-planar molecule

ABSTRACT

Molecular networks connected by halogen bonds have been actively studied due to their ubiquity in biological systems and complementary role to hydrogen bonds. Although networks of planar molecules with halogen ligands have been studied using scanning tunneling microscopy (STM), those of non-planar molecules have not. Here, we report on the network structures of non-planar molecules containing Br-ligands, tetrabromo-spirobifluorene on Au (111), studied using STM. One and two-dimensional networks were observed and their intermolecular interactions were investigated. In two-dimensional networks, a molecule forms 3.5 Br···Br halogen bonds and 2 Br···H hydrogen bonds, as supported by our density functional theory calculation results. Our study demonstrates that intermolecular structures of non-planar molecules with halogen bonds can be probed on surfaces using STM.

1. Introduction

Increasing numbers of organic drug candidate molecules include halogen ligands to boost membrane permeability [1–3]. Halogen ligands have abnormal electrostatic potential distributions; a positive potential region called a σ-hole is surrounded by a negative potential region, showing cylindrical symmetry along the axis of the ligand bond [4–14]. The σ-hole of a halogen ligand attracts the negative potential regions of oxygen, nitrogen, and other halogen ligands, resulting in halogen bonds. Halogen bonds can be as strong as hydrogen bonds, but show different directionality. Thus they are considered as complimentary tools for forming supramolecular structures that can be applied to molecular recognition, storage, and catalysis [8–11]. The networks of supramolecular structures formed with halogen bonds have been actively studied for the last five years using scanning tunneling microscopy (STM) [15–26]. They have been found to form various two-dimensional networks such as square, rectangular, hexagonal, chevron, or parallel-array structures on crystal surfaces. These previous studies have been of planar molecules to guarantee the ease of the identification of single molecules and their interactions, but in nature there are more non-planar molecules than planar ones. As far as we are aware, there has been no STM study of supramolecular structures formed from non-planar molecules through halogen bonding.

Here, we present an STM study of the network structures of tetrabromo-spirobifluorene (TBSBF), a non-planar molecule containing Br-ligands on Au (111). We observed one and two-dimensional networks and proposed their atomistic models. In the two-dimensional networks, a molecule forms 3.5 Br···Br halogen bonds and 2 Br···H hydrogen bonds, according to our density functional theory (DFT) calculations. Our study shows that the network structures and interactions of non-planar molecules with halogen ligands can be successfully revealed using STM on surfaces.

2. Experimental methods

The experiments were performed using a home-built STM housed in an ultrahigh vacuum (UHV) chamber with a base pressure below 1×10^{-10} torr. The Au (111) surface was prepared from a 200 nm thick film of Au on mica that had been exposed to several cycles of Ne-ion sputtering and annealing at 800 K over the course of 1 h. The surface cleanliness of the Au (111) was checked by confirming the typical herringbone structures on the terraces in STM images. Commercially available TBSBF molecules (Tokyo Chemical Industry, Japan) were thermally evaporated onto the surface to form a sub-monolayer coverage from an alumina-coated crucible, maintaining the substrate temperature at 150 K. The molecular sources were outgassed for several hours prior to deposition. Once

* Corresponding author
E-mail address: sjkahng@korea.ac.kr (S.-J. Kahng).

http://dx.doi.org/10.1016/j.apsusc.2017.01.260
0169-4332/

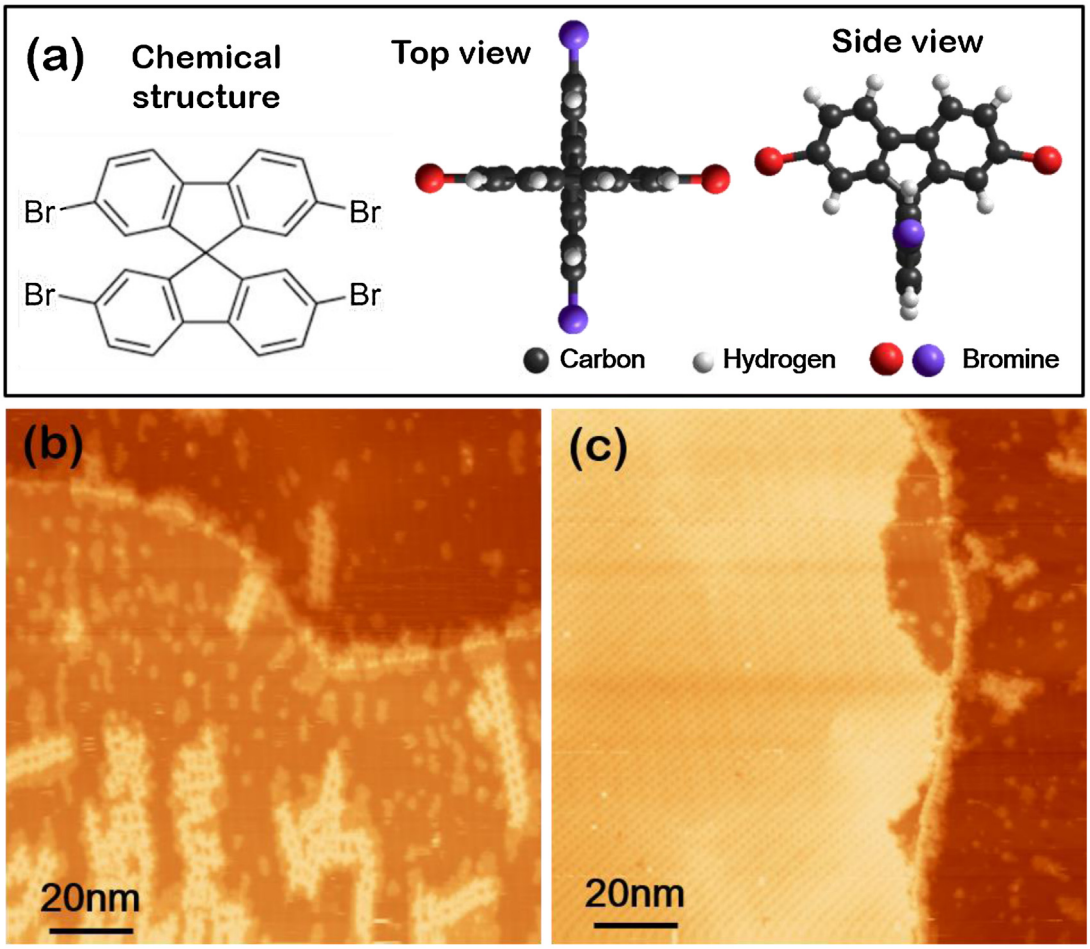

Fig. 1. (a) The chemical structure and the ball and stick 3D model of a TBSBF molecule. (b), (c) Typical STM images of TBSBF molecules on Au (111) surface after heating at (b) 200 K and (c) 300 K. The size of STM images: 128 × 128 nm^2. Tunneling current: I_T = 0.03 nA. Sample voltage: (b) V_S = 0.8 V and (c) V_S = 0.7 V.

prepared, the sample was transferred to the STM, and measured at 80 K using a Pt-Rh alloy tip.

3. Theoretical calculations

DFT calculations were performed using the VASP code [27,28]. Interactions between ions and electrons were approximated by the projector-augmented wave (PAW) potential [29]. The generalized gradient approximation (GGA) with the Perdew-Burke-Ernzerhof (PBE) functional was used to describe the exchange-correlation energies between electrons [30]. The energy cutoff for the plane wave basis was set to 500 eV. To include the non-bonding interactions between the molecules, especially those of the van der Waals type, the empirical scheme proposed by Grimme was adopted [31]. Parallelepiped simulation cells containing two TBSBF molecules were adopted to form the periodic structure. The side lengths *a* and *b* of the parallelogram parallel to the molecular plane were varied to find the most stable structure. The height of the simulation cell perpendicular to the molecular plane was fixed at 50 Å, while the lateral cell parameters *a* and *b* were optimized such that the residual stress was reduced to under 1 kbar.

4. Results and discussion

Fig. 1(a) shows the chemical structure and three-dimensional (3D) ball and stick model of a TBSBF molecule made up of two bibromo-fluorene (BBF) molecules. Two planar BBF molecules share a carbon atom to form a " + "-like non-planar TBSBF structure. When the molecules were deposited at 150 K, rather than forming ordered structures, they formed cluster structures randomly distributed on the terraces. Fig. 1(b), (c) show the STM images obtained at 80 K after depositing the TBSBF molecules on Au (111) at a sub-monolayer coverage and annealing at 200 and 300 K, respectively. After annealing at 200 K, the cluster structures are still visible, and one-dimensional (1D) structures are observed on top of mono-layer islands. However, when the sample was annealed at 300 K, the molecules formed two-dimensional (2D) structures. The 2D structures also formed on top of the mono-layer islands whose structures are not clear from our experiments. It is expected that interaction between the molecules and substrate is marginal. Still, the 2D networks reflect the herringbone structures of Au (111) as shown in Fig. S1(a). The angle between the [1$\bar{2}$1] direction of Au (111) and the direction of a molecular row is estimated to be 30°.

Fig. 2(a)–(d) show higher resolution STM images of the 1D and 2D structures. We considered molecular models in which both BBF planes of the single TBSBF molecules were in 90° configurations with respect to a surface plane. One BBF is close to the surface (the lower BBF), while the other is far from the surface (the upper BBF). A bar-like structure that represents one side of the upper BBF of the TBSBF molecule was regarded as a single molecule. Molecular models are superimposed over the STM images of the 1D structures in Fig. 2(b) and the 2D structures in Fig. 2(d).

To explain the molecular models deduced from our experiments, we calculated the intramolecular electrostatic potential distributions of isolated molecules using DFT calculations. Fig. 3(a)

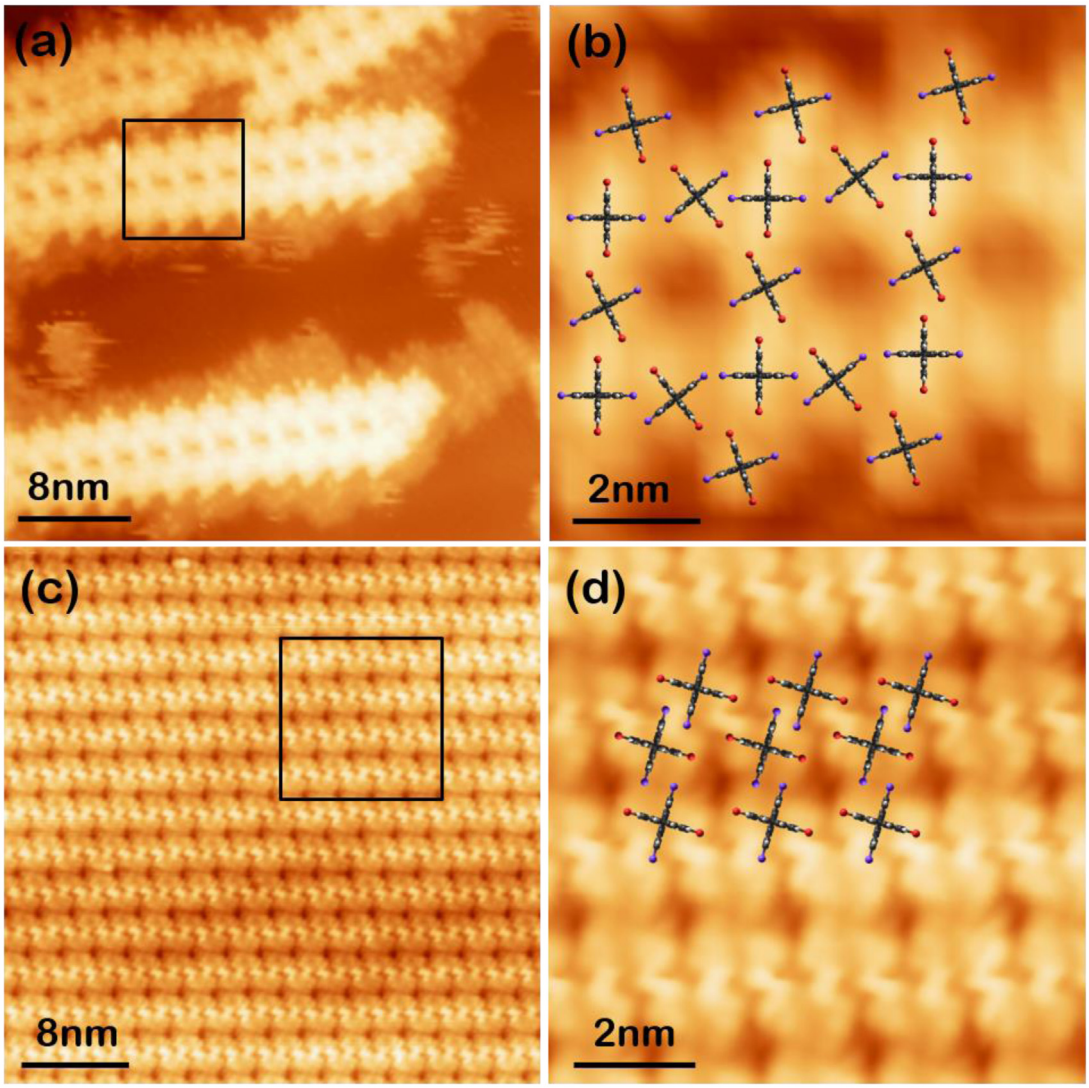

Fig. 2. High resolution (compared to Fig. 1) STM images of (a) and (b) 1D and (c) and (d) 2D structures. STM images of (b) and (d) are magnified from the squared regions in (a) and (c), respectively. Molecular models of TBSBF are superimposed over the STM images of the (b) 1D and (d) 2D structures. The sizes of STM images: (a) $38 \times 38\,nm^2$, (b) $8.4 \times 8.4\,nm^2$, (c) $31 \times 31\,nm^2$ and (d) $9.3 \times 9.3\,nm^2$. Tunneling current: $I_T = 0.03$ nA. Sample voltage: (a) and (b) $V_S = 0.99$ V, (c) $V_S = 0.87$ V, and (d) $V_S = 1.28$ V.

shows the electrostatic potential mapped on isosurfaces of $0.02\,e/Å^3$. H atoms exhibit a positive electrostatic potential while Br atoms exhibit both positive and negative electrostatic potentials with the unique σ-hole structure. As shown in Fig. 3(b), the interactions among the neighboring molecules in the 2D structures can be plotted based on the potential distributions of a single molecule, with a simplified version of the electrostatic potential distributions around the Br and H-ligands. To indicate the distance of Br atoms from the surface, both blue and cyan were used for negative potentials. The blue colored Br is in the upper BBF plane, and the cyan colored Br is in the lower BBF plane. Using these plots, the experimentally-derived models of the 2D structures in Fig. 2(d) can be explained by possible bonds, which are depicted in Fig. 3(b) as colored solid lines for Br···Br halogen bonds and dashed lines for hydrogen bonds. The three Br atoms in a TBSBF molecule may form 3 Br···Br halogen bonds and 2 Br···H hydrogen bonds, and the last Br atom may form a Br···Br halogen bond.

We performed DFT calculations to explain the detailed intermolecular configurations of the 2D structures. Parallelogram unit cells containing two TBSBF molecules were used to construct the periodic structures depicted in Fig. 4(a). We considered the side lengths (a, b) and the angle θ of the parallelogram as three independent parameters. In Fig. 4(b) the calculated formation energy is represented by color as a function of a and b at an angle of 72°. Zero energy would correspond to the energy of an isolated molecule. As we varied the angle away from 72°, the formation energy always increased for any set of (a, b). The most stable structure had $a = 1.32$ and $b = 1.67$ nm, and this finding was in reasonable agreement with the experimentally observed values of $a = 1.40 \pm 0.1$ nm and $b = 1.75 \pm 0.1$ nm.

Using the minimum-energy structures in Fig. 4, the distances of the possible halogen bonds and hydrogen bonds in Fig. 3(b) are determined. The lengths of the possible Br···Br halogen bonds depicted by the pink, green, blue and purple solid lines were 0.36, 0.39, 0.42, and 0.44 nm, respectively. Because the sum of the van der Waals radii is 0.39 nm, the last two should be considered as very weak or marginal halogen bonds. The lengths of the possible Br···H hydrogen bonds depicted as red and cyan dotted lines were 0.29 and 0.34 nm, respectively. The sum of van der Waals radii of Br and H is 0.30 nm. Overall, the molecular structures were stabilized by 3.5 Br···Br halogen bonds and 2 Br···H hydrogen bonds per molecule. If we count only the strong bonds that are shorter than the sum of the van der Waals radii, the molecular structures would be stabilized by 2 Br···Br halogen bonds and 1 Br···H hydro-

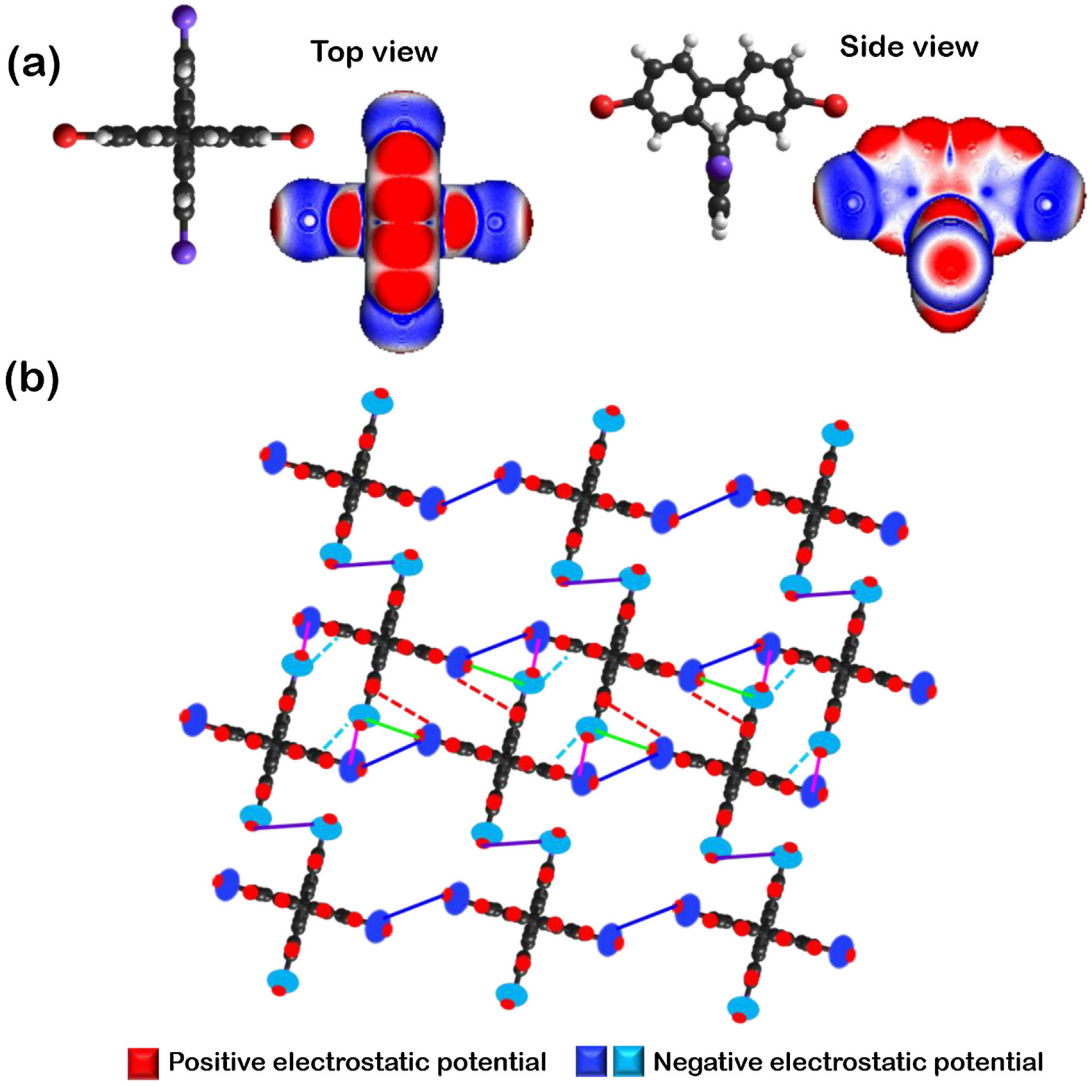

Fig. 3. (a) Calculated electrostatic potential distributions of a TBSBF molecule at isodensity surfaces. (b) Schematic illustrations of neighboring molecules in 2D structures with simplified electrostatic potential distributions around the Br and H atoms. The positive potentials are colored red, and the negative potentials are blue (Br atom in the upper BBF plane) or cyan (Br atom in the lower BBF plane). The solid and dashed lines indicate possible halogen and hydrogen bonds, respectively.

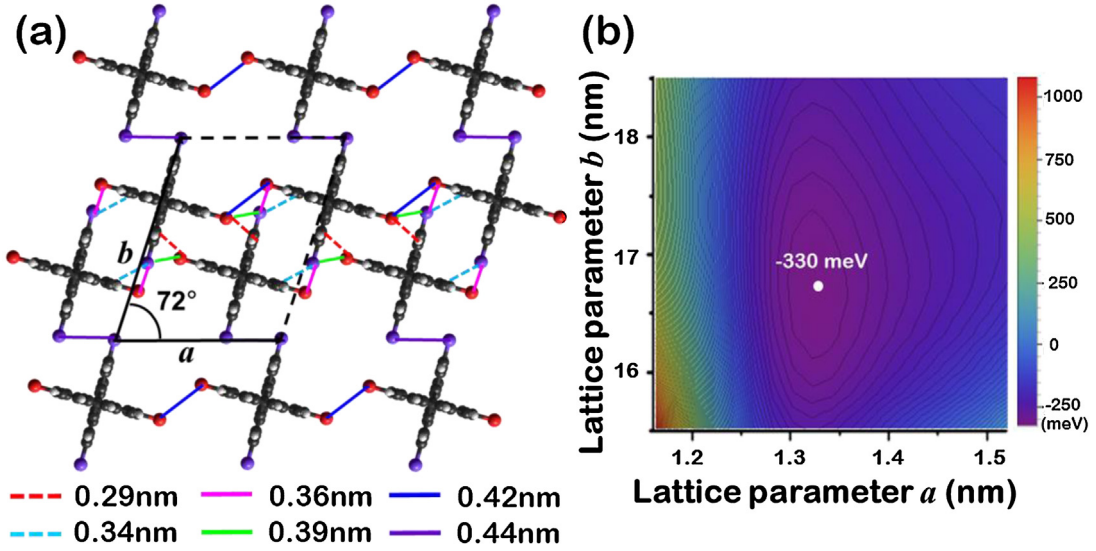

Fig. 4. (a) The calculated results for relaxed 2D structures of TBSBF molecules from DFT calculations. (b) The energy gain per molecule as a function of the lattice parameters *a*, *b* for 2D structures with an angle of 72°.

gen bond per molecule. According to the DFT calculation results, the formation energy was 330 meV per molecule, meaning that the strength of each bond is about 110 meV. Here we considered only the 2D structures using DFT, because the 1D structure was much more complicated.

5. Conclusions

We studied the 1D and 2D structures of non-planar TBSBF on Au (111) using STM. Molecular models of the 2D structures were proposed and explained on the basis of DFT calculations. The 2D structures were stabilized by 3.5 Br···Br halogen bonds and 2 Br···H hydrogen bonds per molecule. Our study shows that the intermolecular structures of non-planar molecules with halogen bond can be probed on surfaces using STM.

Acknowledgments

The authors gratefully acknowledge financial support from the National Research Foundation of Korea (Grant nos. 2012-01013222; 2014-11051782). This work was supported by the Supercomputing Center/Korea Institute of Science and Technology Information with supercomputing resources including technical support (KSC-2015-C1-028).

Appendix A. Supplementary data

Supplementary data associated with this article can be found, in the online version, at http://dx.doi.org/10.1016/j.apsusc.2017.01.260.

References

[1] M.Z. Hernandes, S.M.T. Cavalcanti, D.R.M. Moreira, W.F. de Azevedo, A.C.L. Leite, Halogen atoms in the modern medicinal chemistry: hints for the drug design, Curr. Drug Targets 11 (2010) 303–314.
[2] C.L. Leite, D.R.M. Moreira, M.V.O. Cardoso, M.Z. Hernandes, V.R.A. Pereira, R.O. Silva, A.C. Kiperstok, M.S. Lima, M.B.P. Soares, Synthesis cruzain docking, and in vitro studies of aryl-4-Oxothiazolylhydrazones against trypanosoma cruzi, Chem. Med. Chem. 2 (2007) 1339–1345.
[3] G. Gerebtzoff, X. Li-Blatter, H. Fischer, A. Frentzel, A. Seelig, Halogenation of drugs enhances membrane binding and permeation, Chem. Bio. Chem. 5 (2004) 676–684.
[4] Hassel, Structural aspects of interatomic charge-transfer bonding, O, Science 170 (1970) 497–502.
[5] P. Metrangolo, G. Resnati, H.D. Arman, Halogen Bonding: Fundamental and Applications, Springer-Verlag, Berlin, 2008.
[6] G.R. Desiraju, R. Parthasarathy, The nature of halogen···halogen interactions: are short halogen contacts due to specific attractive forces or due to close packing of nonspherical atoms? J. Am. Chem. Soc. 111 (1989) 8725–8726.
[7] P. Metrangolo, F. Meyer, T. Pilati, G. Resnati, G. Terraneo, Halogen bonding in supramolecular chemistry, Angew. Chem. Int. Ed. 47 (2008) 6114–6127.
[8] P. Metrangolo, G. Resnati, Halogen versus hydrogen, Science 321 (2008) 918–919.
[9] R. Paulini, K. Müller, F. Diederich, Orthogonal multipolar interactions in structural chemistry and biology, Angew. Chem. Int. Ed. 44 (2005) 1788–1805.
[10] J. Navon, V. Bernstein, Chains Khodorkovsky, Ladders, and two-dimensional sheets with Halogen···Halogen and Halogen···Hydrogen interactions, Angew. Chem. Int. Ed. 36 (1997) 601–603.
[11] H.F. Lieberman, R.J. Davey, D.M.T. Newsham, Br···Br and Br···H interactions in action: polymorphism, hopping and twinning in 1 2, 4, 5-Tetrabromobenzene, Chem. Mater. 12 (2000) 490–494.
[12] Corinne L.D. Gibb, Edwin D. Stevens, Bruce C. Gibb, C-H··X-R (X = Cl, Br, and I) hydrogen bonds drive the complexation properties of a nanoscale molecular basket, J. Am. Chem. Soc. 123 (2001) 5849–5850.
[13] E. Corradi, S.V. Meille, M.T. Messina, P. Metrangolo, G. Resnati, Halogen bonding versus hydrogen bonding in driving self-assembly processes, Angew. Chem. Int. Ed. 39 (2000) 1782–1786.
[14] C.B. Aakeröy, M. Fasulo, N. Schultheiss, J. Desper, C. Moore, Structural competition between hydrogen bonds and halogen bonds, J. Am. Chem. Soc. 129 (2007) 13772–13773.
[15] H. Walch, R. Gutzler, T. Sirtl, G. Eder, M. Lackinger, Material- and orientation-dependent reactivity for heterogeneously catalyzed carbon-bromine bond homolysis, J. Phys. Chem. C. 114 (2010) 12604–12609.
[16] J.K. Yoon, W.-J. Son, K.-H. Chung, H. Kim, S. Han, S.-J. Kahng, Visualizing halogen bonds in planar supramolecular systems, J. Phys. Chem. C. 115 (2011) 2297–2301.
[17] J.K. Yoon, W.-J. Son, H. Kim, K.-H. Chung, S. Han, S.-J. Kahng, Achieving chiral resolution in self-assembled supramolecular structures through kinetic pathways, Nanotechnology 22 (2011) 275705.
[18] J.C. Russell, M.O. Blunt, J.M. Garfitt, D.J. Scurr, M. Alexander, N.R. Champness, P.H. Beton, Dimerization of tri(4-bromophenyl)benzene by aryl-aryl coupling from solution on a gold surface, J. Am. Chem. Soc. 133 (2011) 4220–4223.
[19] R. Gutzler, O. Ivasenko, Ch. Fu, J.L. Brusso, F. Rosei, D.F. Perepichka, Halogen bonds as stabilizing interactions in a chiral self-assembled molecular monolayer, Chem. Commun. 47 (2011) 9453–9455.
[20] K.-H. Chung, J. Park, K.Y. Kim, J.K. Yoon, H. Kim, S. Han, S.-J. Kahng, Polymorphic porous supramolecular networks mediated by halogen bonds on Ag(111), Chem. Commun. 47 (2011) 11492–11494.
[21] S.-K. Noh, J.H. Jeon, W.J. Jang, H. Kim, S.-H. Lee, M.W. Lee, J. Lee, S. Han, S.-J. Kahng, Supramolecular Cl···H and O··H interactions in self-Assembled 1, 5-Dichloroanthraquinone layers on Au (111), Chem. Phys. Chem. 14 (2013) 1177–1181.
[22] W.-J. Jang, K.H. Chung, M.W. Lee, H. Kim, S.J. Lee, S.-J. Kahng, Tetragonal porous networks made by rod-like molecules on Au (111) with halogen bonds, Appl. Surf. Sci. 309 (2014) 74–78.
[23] D. Peyrot, F. Silly, On-Surface synthesis of two-dimensional covalent organic structures versus halogen-Bonded self-assembly: competing formation of organic nanoarchitectures, ACS Nano 10 (2016) 5490–5498.
[24] T.T.T. Bui, S. Dahaoui, C. Lecomte, G.R. Desiraju, E. Espinosa, The nature of Halogen···Halogen interactions: a model derived from experimental charge-Density analysis, Angew. Chem. Int. Ed. 48 (2009) 3838–3841.
[25] R.H. Venkatesha, T.N. Guru Row, Nature of Cl···Cl intermolecular interactions via experimental and theoretical charge density analysis: correlation of polar flattening effects with geometry, J. Phys. Chem. A 114 (2010) 13434–13441.
[26] R. Wang, T.S. Dols, C.W. Lehmann, U. Englert, The halogen bond made visible: experimental charge density of a very short intermolecular Cl···Cl donor?acceptor contact, Chem. Commun. 48 (2012) 6830–6832.
[27] G. Kresse, J. Hafner, Ab initio molecular dynamics for liquid metals, Phys. Rev. B. 47 (1993) 558–561.
[28] G. Kresse, J. Hafner, Ab initio molecular-dynamics simulation of the liquid-metal–amorphous-semiconductor transition in germanium, Phys. Rev. B 49 (1994) 14251–14269.
[29] P.E. Blöchl, Projector augmented-wave method, Phys. Rev. B. 50 (1994) 17953–17979.
[30] J.P. Perdew, K. Burke, M. Ernzerhof, Generalized gradient approximation made simple, Phys. Rev. Lett. 77 (1996) 3865–3868.
[31] S. Grimme, Accurate description of van der Waals complexes by density functional theory including empirical corrections, J. Comput. Chem. 25 (2004) 1463–1473.